

SUPPORTING INFORMATION

(17 pages containing 16 supplemental figures)

Programming post-translational control over the metabolic labeling of cellular proteins with a non-canonical amino acid

Emily E. Thomas^{1,2}, Naresh Pandey¹, Sarah Knudsen³, Zachary T. Ball³, and Jonathan J. Silberg^{1,4*}

Author affiliations:

1. Department of Biosciences, Rice University, Houston, TX 77005, USA
2. Biochemistry and Cell Biology Graduate Program, Rice University, Houston, TX 77005, USA
3. Department of Chemistry, Rice University, Houston, TX 77005, USA
4. Department of Bioengineering, Rice University, Houston, TX 77005, USA

*Address correspondence to:

Dr. Jonathan Silberg
6100 Main Street, Houston, TX 77005
Phone: 713-348-3849; Fax: 713-348-5154
Email: joff@rice.edu

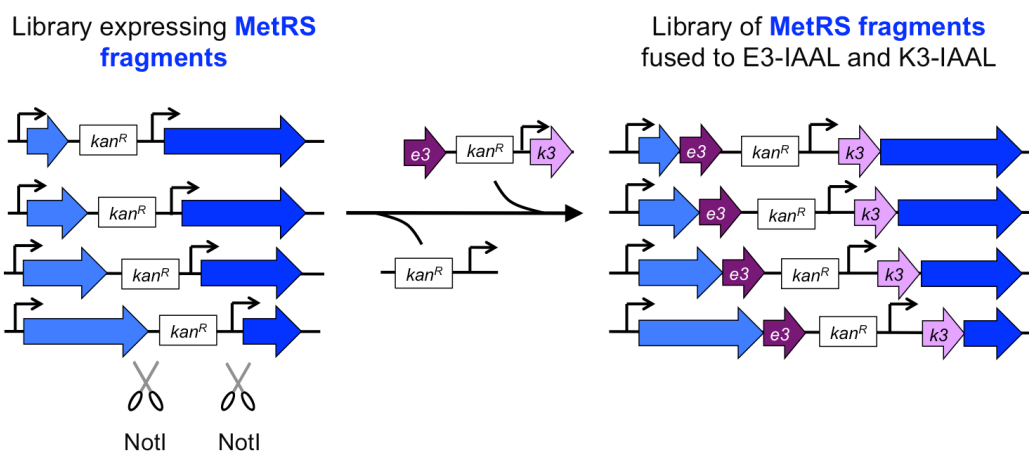


Figure S1. Scheme illustrating vector library construction. A library previously constructed¹⁸ to express split MetRS lacking peptide fusions was digested with NotI to remove *f1-kan^R*, the DNA insert that encodes the stop codon terminating translation of the N-terminal fragment and the promoter and RBS that initiates translation of the C-terminal fragment. This DNA was replaced with *ek-kan^R* to create vectors that express different two-fragment MetRS variants in which the first protein fragment is expressed as a fusion to IAAL-E3 and the second protein fragment is expressed as a fusion to IAAL-K3.

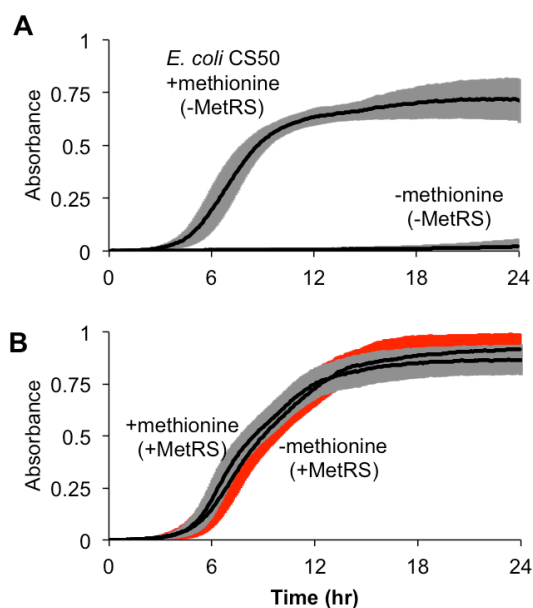


Figure S2. Assessing MetRS activity using *E. coli* CS50 complementation. The absorbance at 600 nm of *E. coli* CS50 cells transformed with (A) an empty vector and (B) a vector that constitutively expresses MetRS was analyzed in minimal medium containing or lacking methionine. Cell growth was performed at 37°C. The bold line represents the average of 42 experiments, and the shaded area represents $\pm 1\sigma$.

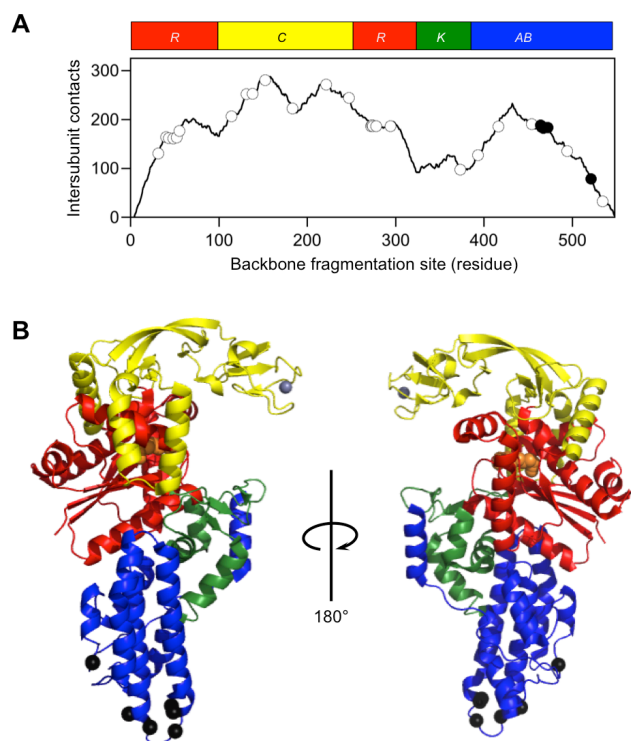


Figure S3. Structural model for two-fragment MetRS. (A) The number of intermolecular contacts made between fragments in every possible split MetRS are mapped onto the connective polypeptide (CP), Rossmann fold (R), KMSKS (K), and anticodon-binding (AB) domains. The fragmented MetRS that are active when fused to EK coils (●) are compared with split MetRS that lack fusions to peptides that associate (○), which were reported in a previous study.¹⁸ (B) The backbone cleavage sites (black spheres) that yielded each functional split MetRS are mapped onto the MetRS structure, which is color coded by domain. Calculations were performed as previously described.¹⁸

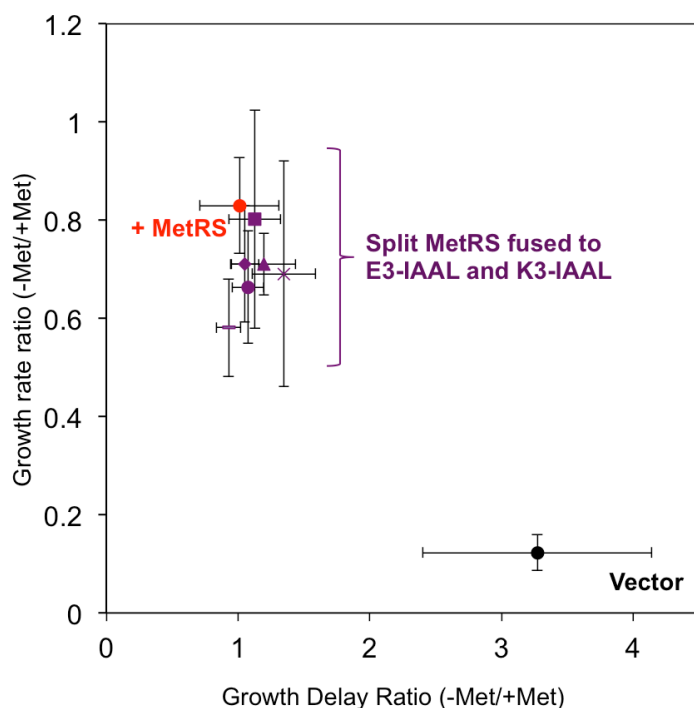


Figure S4. *E. coli* CS50 complementation by MetRS fragments fused to IAAL-E3 and IAAL-K3. The ratio of growth rates and delays in the absence and presence of methionine for MetRS-464 (–), MetRS-465 (×), MetRS-467 (■), MetRS-470 (◆), MetRS-472 (▲), and MetRS-521 (●). As a frame of reference, we report the growth of *E. coli* CS50 in the presence of a non-bisected MetRS (●) and empty vector (●). Ratio calculations used the largest rate achieved during the incubation at 37°C while delay is the average length of time required for cultures to reach exponential growth. For each split MetRS, the error bars represent the standard deviation from six experiments performed using distinct colonies, while the error bars for the controls represent the standard deviation from 24 distinct colonies. Only a subset of the experiments involving the empty vector yielded sufficient growth to estimate the rate and delay. For this reason, this data represents a lower bound for delay and upper bound for rate.

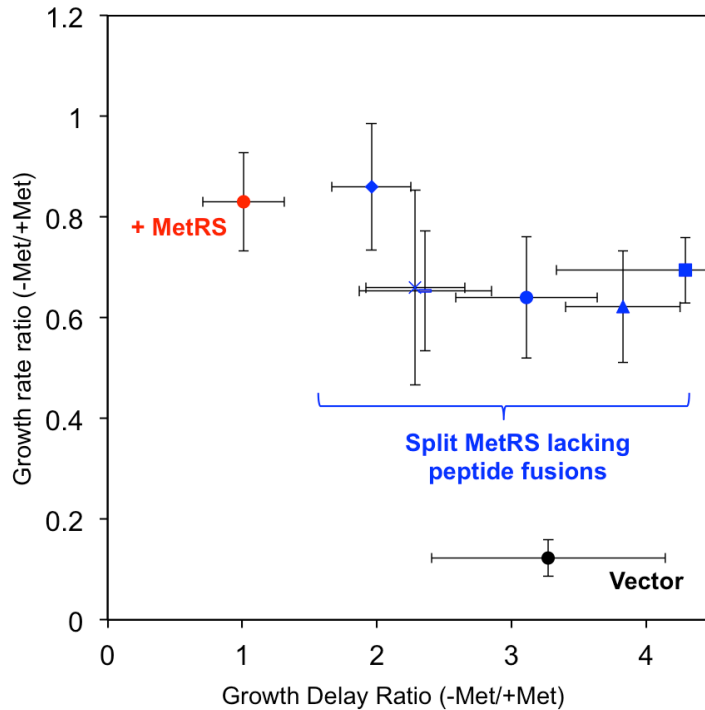


Figure S5. *E. coli* CS50 complementation by MetRS fragments lacking fusions.

The ratio of growth rates and delays in the absence and presence of methionine for MetRS-464 (–), MetRS-465 (×), MetRS-467 (■), MetRS-470 (◆), MetRS-472 (▲), and MetRS-521 (●). As a frame of reference, we report the growth of *E. coli* CS50 in the presence of a non-bisected MetRS (●) and empty vector (●). Ratio calculations used the largest rate achieved during the incubation at 37°C while delay is the average length of time required for cultures to reach exponential growth. For each split MetRS, the error bars represent the standard deviation from six experiments performed with distinct colonies, while the error bars for the controls are the standard deviation from 24 distinct colonies. Only a subset of the experiments involving the empty vector yielded sufficient growth to estimate the rate and delay. For this reason, the empty vector data represents a lower bound for delay and upper bound for rate.

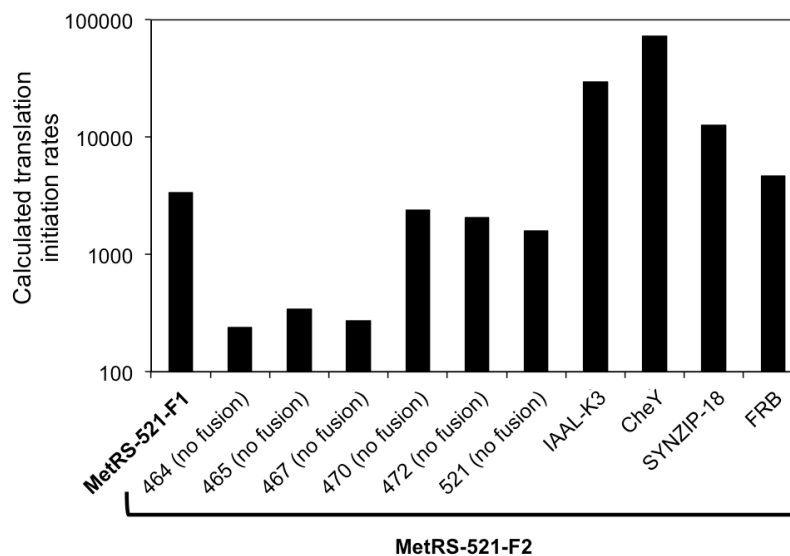


Figure S6. Translation initiation calculated using a thermodynamic model.³⁵ For each fragment in our different split MetRS, we analyzed whether the translation initiation rates varied when the N-terminal MetRS fragments (F1) and C-terminal MetRS fragments (F2) were expressed alone or as fusions to the indicated proteins. The translation initiation of the first fragment is predicted to be the same in all vectors because the genetic context of the RBS does not change. In this model, the genetic context of an RBS is used to estimate the relative strengths of mRNA-ribosome binding that underlies translation initiation and RNA folding that inhibits mRNA-ribosome binding. Forward engineering experiments have revealed that this model is accurate within a factor of 2.3-fold over translation initiation values spanning 5 orders of magnitude.³⁵

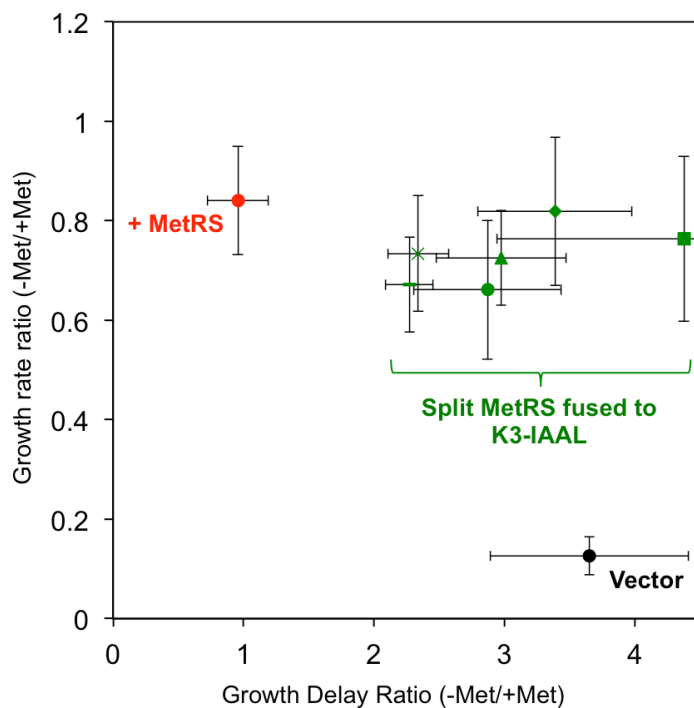


Figure S7. *E. coli* CS50 complementation by split MetRS having only the C-terminal fragment fused to IAAL-K3. To disrupt the peptide interaction without altering translation initiation, we analyzed the ratio of growth rates and delays in the absence and presence of methionine for MetRS-464 (–), MetRS-465 (×), MetRS-467 (■), MetRS-470 (◆), MetRS-472 (▲), and MetRS-521 (●). As a frame of reference, we report the growth of *E. coli* CS50 in the presence of a non-bisected MetRS (●) and empty vector (●). Growth rate represents the largest rate achieved during the incubation at 37°C while delay is the average length of time required for cultures to reach exponential growth. For each split MetRS, the error bars represent the standard deviation from six samples derived from distinct colonies, while the error bars for the controls are the standard deviation from 24 distinct colonies. Only a subset of the experiments involving the empty vector yielded sufficient growth to estimate the rate

and delay. For this reason, the empty vector data represents a lower bound for delay and upper bound for rate.

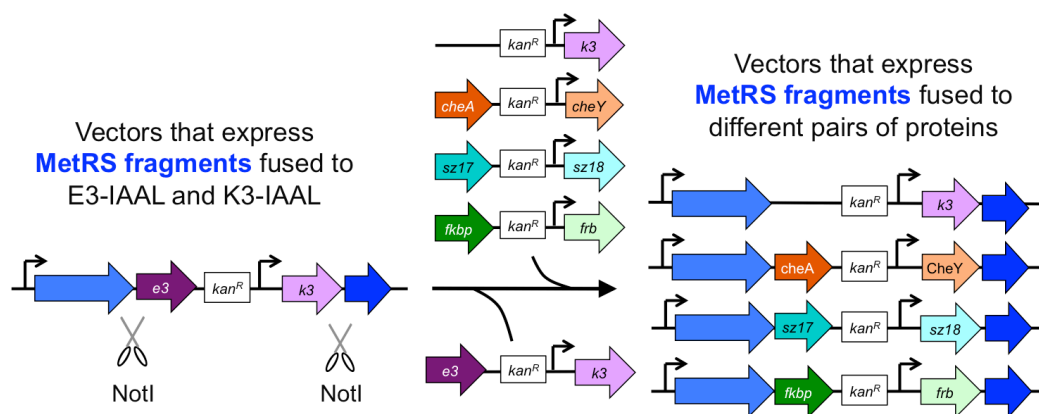


Figure S8. Scheme illustrating vector one-step vector modification to alter the pair of proteins fused to MetRS fragments. In the vectors created in our library, a pair of NotI sites flanks the DNA insert (*ek-kan^R*) that separates the open reading frames encoding each MetRS fragment (blue), which encodes the IAAL-E3 and IAAL-K3 peptides that are amended to the termini of each MetRS fragment. This DNA insert can be removed through NotI digestion and replaced with inserts encoding different pairs of interacting proteins, such as CheA and CheY (*ay-kan^R*), SYNZIP-17 and SYNZIP-18 (*sz-kan^R*), FKBP and FRB (*ff-kan^R*), and IAAL-K3 (*k-kan^R*).

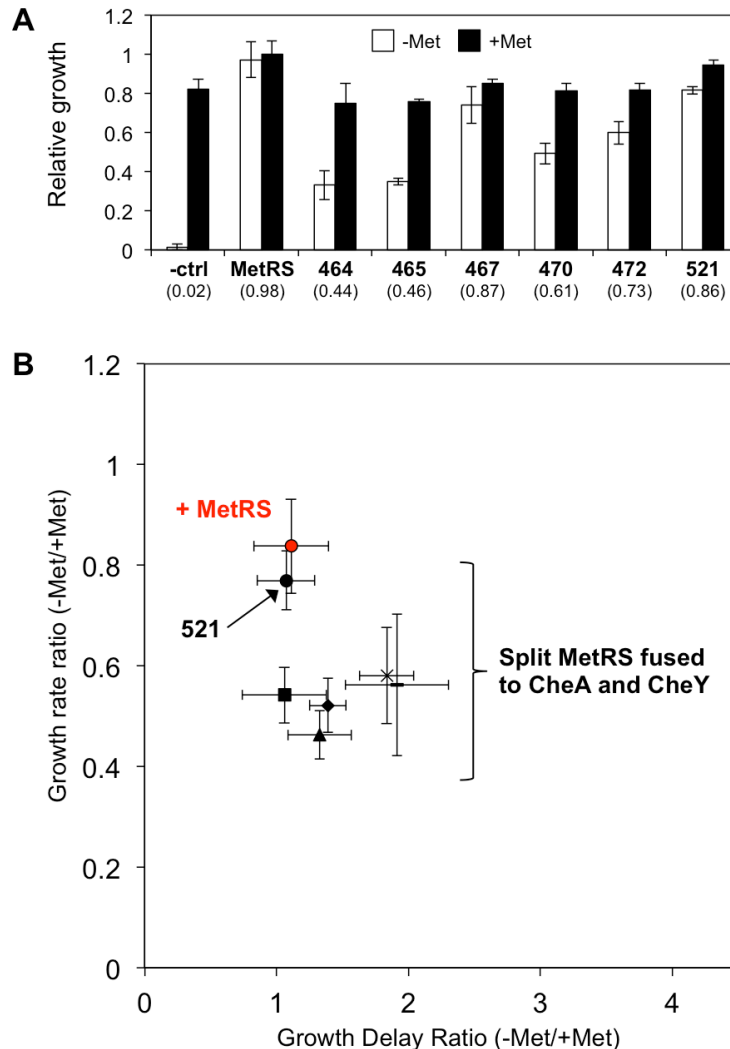


Figure S9. *E. coli* CS50 complementation by split MetRS fused to CheA and CheY. (A) For each variant, the relative growth was calculated as the area under the growth curve over a 24 hour incubation in minimal medium lacking (open bars) and containing supplemental methionine (closed bars). The values below each pair of bars represent the ratio of growth in the absence and presence of methionine. The growth ratio was significantly increased in three of the variants (MetRS 467, 472, and 521) compared to MetRS lacking peptide fusion ($p < 0.05$, two-tailed t test). (B) The ratio of growth rates and delays in the absence and presence of methionine for MetRS-464 (–), MetRS-465 (x), MetRS-467 (■), MetRS-470 (◆), MetRS-472 (▲), and MetRS-521 (●). As a frame of reference, we show the growth of *E. coli* CS50 in the presence of a non-bisected MetRS (●). For each split MetRS, the error bars represent the standard deviation from 6 experiments performed using distinct colonies. Among the six split MetRS, the

MetRS-521 complementation was most similar to the MetRS control across all growth metrics evaluated.

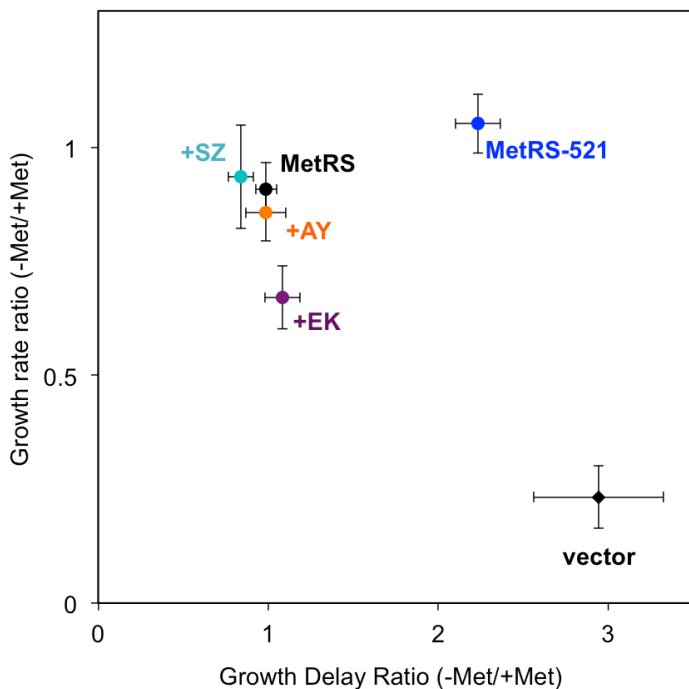


Figure S10. Effect of varying protein fusions on MetRS-521 complementation. The ratio of growth rates and delays in the absence and presence of methionine for MetRS-521 lacking protein fusions (MetRS-521) and having its fragments fused to IAAL-E3 and IAAL-K3 (+EK), CheA and CheY (+AY), SYNZIP-17 and SYNZIP-18 (+SZ). Growth rate represents the largest rate achieved during the incubation at 37°C while delay is the average length of time required for cultures to reach exponential growth. For each experiment, the error bars represent the standard deviation from 8 samples. Only a subset of the experiments involving the empty vector yielded sufficient growth to estimate the rate and delay. For this reason, the empty vector data represents a lower bound for delay and upper bound for rate.

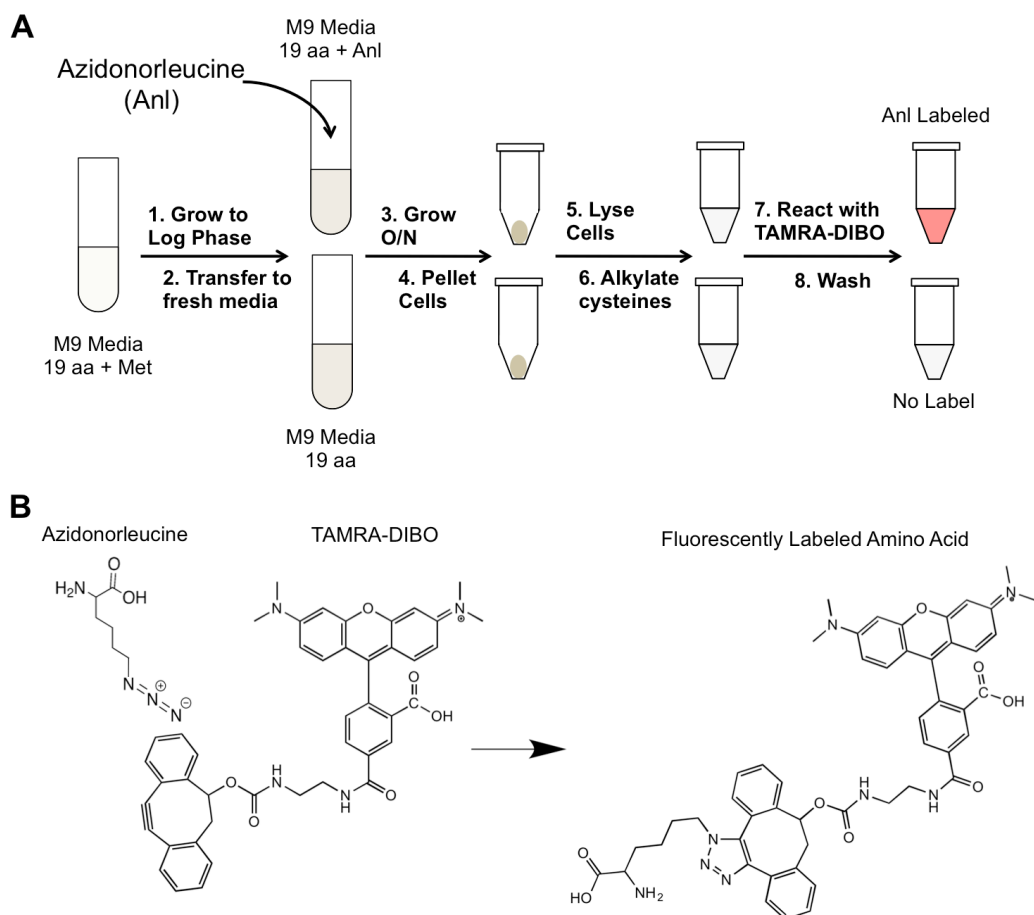


Figure S11. Protocol used to detect azide-labeled proteins. (A) *E. coli* transformed with vectors that express NLL-MetRS and different NLL-MetRS-521 variants were grown overnight to stationary phase in minimal medium containing methionine. These cultures were then used to seed a fresh culture, which was grown to mid log phase and split into two cultures, one containing and one lacking azidonorleucine. These cultures were grown overnight to allow for Anl metabolic labeling. To visualize labeling, cells were lysed and treated with iodoacetamide to alkylate cysteines. The alkylated proteins were then precipitated, resuspended in TBS, and incubated with TAMRA-DIBO at room temperature for one hour. The resulting TAMRA-labeled proteins were precipitated and resuspended in TBS prior to analyzing their fluorescence. **(B)** The azide of the azidonorleucine reacts with the cyclooctyne strained ring of the TAMRA-DIBO dye via a [3+2] cycloaddition to create a fluorescently tagged amino acid.

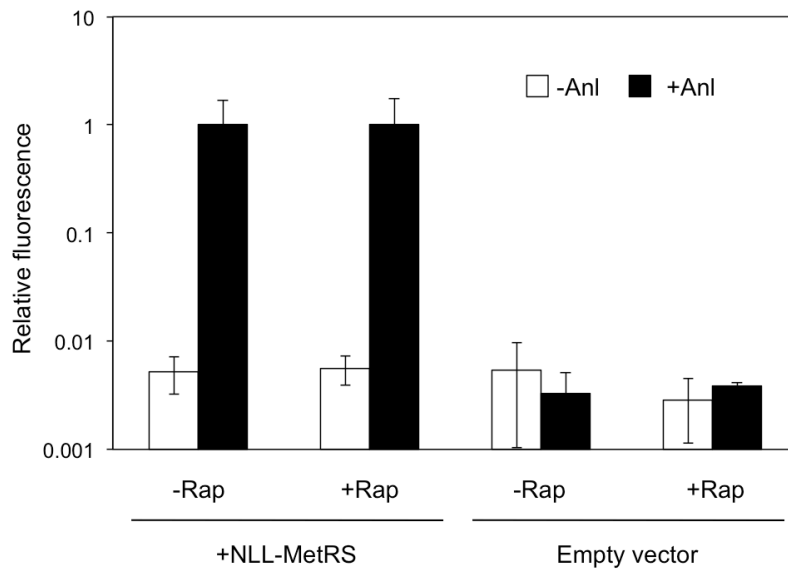


Figure S12. Rapamycin does not affect metabolic labeling by NLL-MetRS. Protein-normalized TAMRA fluorescence was measured in cell lysates that were derived from cells that had been grown in the presence and absence of rapamycin (10 μ M) and Anl (2 mM). Experiments were performed using cells that had been transformed with a vector that expresses NLL-MetRS or an empty vector, and all samples were induced with 100 μ M IPTG. The error bars represent the standard deviation from three different experiments.

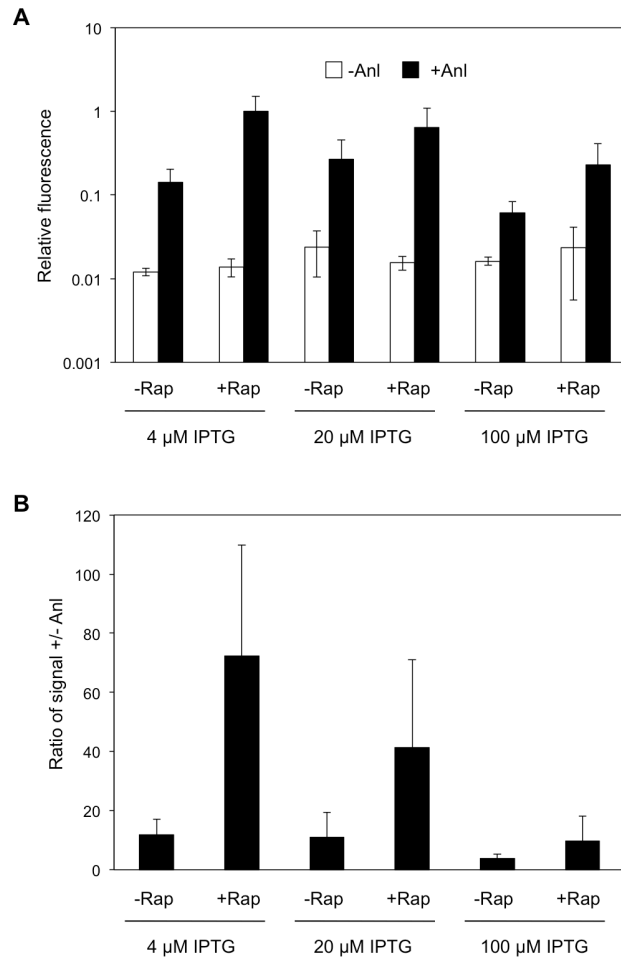


Figure S13. The effect of varying IPTG on rapamycin-induced metabolic labeling. Protein-normalized TAMRA fluorescence was measured in cell lysates that were derived from cells that expressed NLL-MetRS-521 fragments as fusions to FKBP and FRB. Experiments were performed using a range of IPTG concentrations in the presence and absence of rapamycin (10 μ M) and Anl (2 mM). The error bars represent the standard deviation from three different experiments.

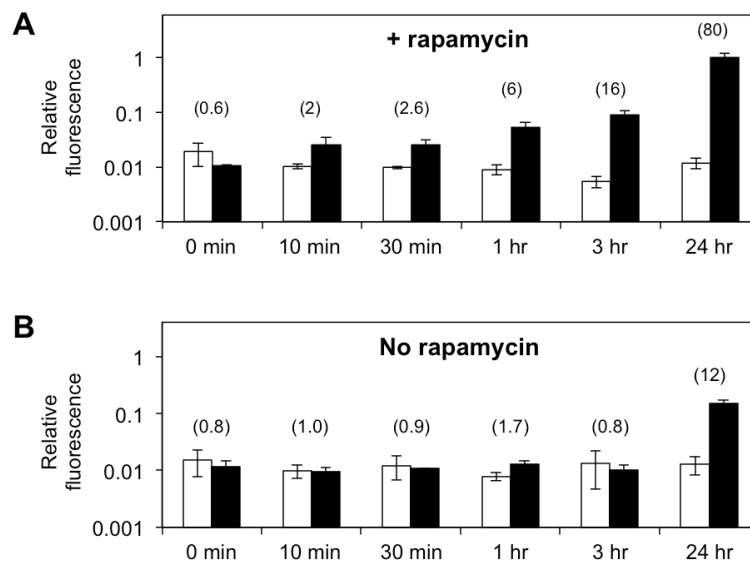


Figure S14. AnI labeling at different times following rapamycin addition. Identical titers of cells containing the vector that expresses NLL-MetRS-521 fragments fused to FKBP and FRB were used to seed cultures containing (closed bars) or lacking AnI (open bars). Parallel cultures derived from the same cells were set up that (A) contained 10 μ M rapamycin or (B) lacked rapamycin. At different times following inoculation, cells were harvested, labeling was visualized using fluorescence, total protein was measured, and protein-normalized fluorescence was calculated. For each construct, the ratio of fluorescence \pm AnI is provided above the bars. Rapamycin addition yielded fluorescence significantly greater than the no AnI background after 30 minutes ($p < 0.05$, two-tailed Welch's t test). The error bars represent $\pm 1\sigma$ from three experiments for all

conditions except the -AnI experiments containing (30 min 3 hour) and lacking (0 min) rapamycin where two experiments were performed.

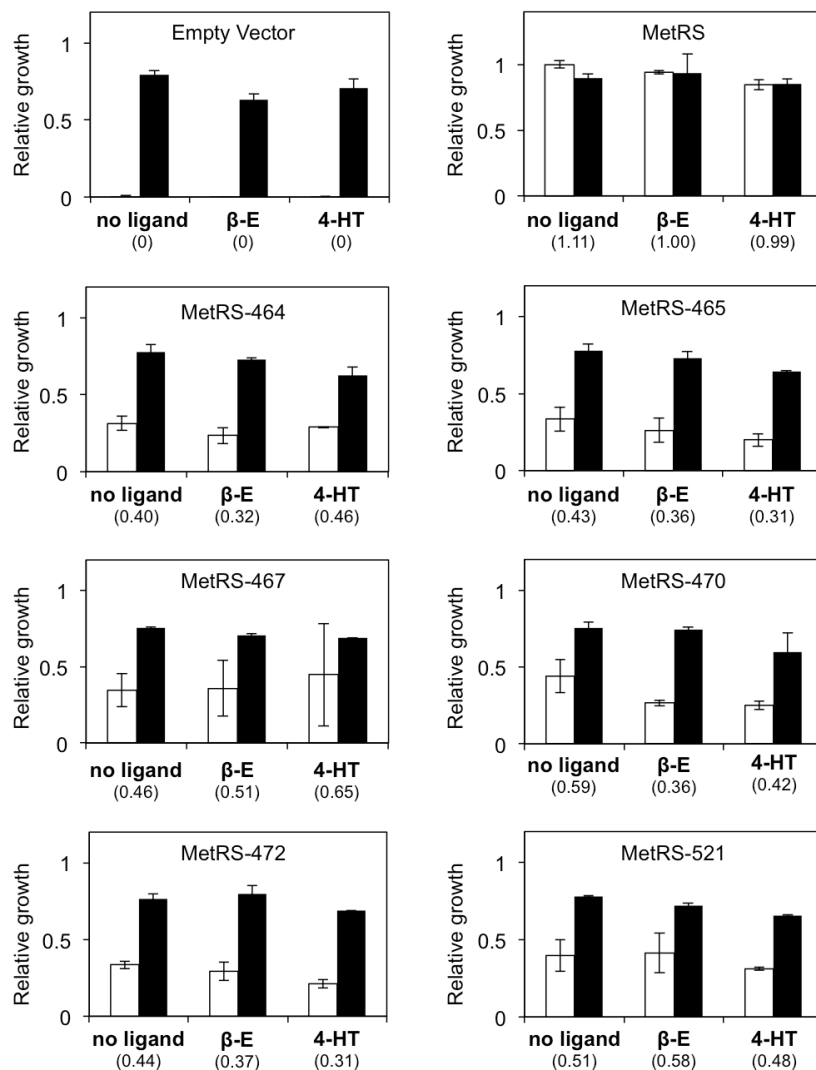


Figure S15. Effect of domain insertion on MetRS activity. *E. coli* CS50 transformed with vectors that express MetRS having the ER LBD inserted at different sites (after residues 464, 465, 467, 470, 472, and 521) were grown in minimal medium lacking (open bars) or containing (closed bars) methionine. As controls, we also transformed cells with an empty ligand and a vector that expresses MetRS. After a 24 hour incubation, the relative growth was calculated as the area under the growth curve over the full incubation time. The values listed below the bars represent the ratio of growth in the absence of methionine to the growth in the presence of methionine. The concentrations of β -E and 4-HT were both 100 μ M. Error bars represent $\pm 1\sigma$ calculated

from two experiments. All growth is normalized to that observed with cells expressing MetRS in the absence of methionine.

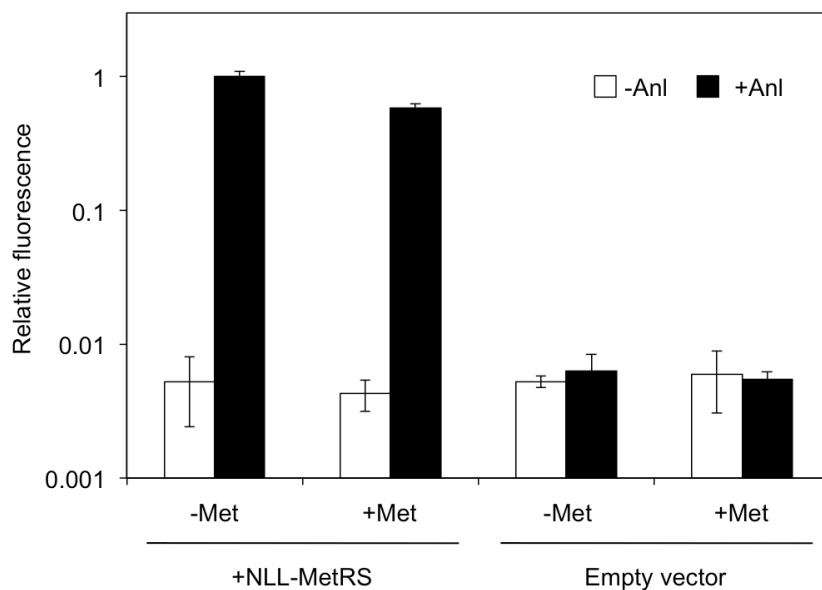


Figure S16. Anl metabolic labeling is not affected by methionine addition. Cells transformed with a plasmid that expresses NLL-MetRS or an empty vector were grown in M9 media supplemented with Anl (2 mM) and either 19 amino acids (-Met) or all twenty amino acids (+Met). Labeling was visualized by reacting cell lysates from each culture with TAMRA-DIBO and measuring fluorescence, the Bio-Rad Protein Assay was used to determine total protein in each sample, and the relative signal was calculated as the protein-normalized fluorescence. The signals obtained in the presence of Anl (closed bars) were compared with those obtained in the absence of Anl (open bars) to obtain the metabolic labeling arising from expressing NLL-MetRS. No significant

difference in the relative fluorescence \pm AnI was observed between experiments performed using growth medium \pm Met with cells expressing NLL-MetRS (left; $p=0.5$) or containing an empty vector (right; $p=0.5$).